Hindawi
International Journal of Geophysics
Volume 2023, Article ID 2186857, 20 pages
https://doi.org/10.1155/2023/2186857

Research Article

Climate Change Impact on the Trigger of Natural Disasters over South-Eastern Himalayas Foothill Region of Myanmar: Extreme Rainfall Analysis

Kyaw Than Oo[1,2] **Chen Haishan**[1] **and Kazora Jonah**[1,3]

[1]*School of Atmospheric Sciences, Nanjing University of Information Science and Technology, Nanjing, China*
[2]*Aviation Weather Services, Yangon, Myanmar*
[3]*Rwanda Meteorology Agency (Meteo Rwanda), Kigali, Rwanda*

Correspondence should be addressed to Kyaw Than Oo; kyawthanoo34@outlook.com

Received 30 August 2023; Revised 20 November 2023; Accepted 6 December 2023; Published 22 December 2023

Academic Editor: Sampad Kumar Panda

The study examines the characteristics and variability of monsoon rainfall in Myanmar, focusing on the relationship between heavy rainfall, floods, and earthquakes, which impact agriculture, hydrology, and the environment. Generally, heavy rainfall can cause flooding, economic losses, and water table changes. Northern Myanmar floods occur mainly during the monsoon season from June to October and can be classified into widespread floods along major rivers like Ayeyarwady, Thanlwin, Chindwin, and Sittoung and flash floods in small streams and rivers. Climate change is expected to increase the frequency and intensity of extreme weather events, including heavy rainfall, which can trigger floods or landslides, which also can in turn cause earthquakes. Heavy rainfall over northern Myanmar and the Sagaing faults, which are the main triggers of earthquakes, has been the subject of several studies. The study uses the Copernicus 5 database of global climate model (GCM) simulations with two scenario analyses on climate change detection and indices (ETCCDI) to study changes in climatic extremes. Results show high intensity in the northern region and monsoon core regions, while the central region shows less intensity. The study also uses intensity-duration-frequency (IDF) curves to analyze the relationship between rainfall duration, intensity, and return time in major risk zones. The study finds that as short duration lengthens, rainfall intensity increases for future rainfall patterns. This information is expected to be convenient for local authorities and flood protection projects in rural and urban basins.

1. Introduction

Myanmar, located in Southeast Asia, experiences a monsoon climate characterized by distinct wet and dry seasons. The country's monsoon season generally lasts from May to October, with the highest rainfall occurring in July and August. Monsoon rainfall is critical to Myanmar's agriculture sector, which is the primary source of livelihood for the majority of the population. During this time, heavy rains replenish the soil, recharge groundwater, and provide water for irrigation. This is crucial for rice cultivation, which is the main crop in Myanmar and a major source of income for many farmers. Several studies have examined the characteristics and variability of monsoon rainfall in Myanmar. For instance, the studies by Mie et al. and Oo analyzed the spatial and temporal patterns of monsoon rainfall in Myanmar between 1981 and 2020 [1–3]. These studies found that monsoon rainfall in Myanmar exhibited significant variability at both spatial and temporal scales, with pronounced interannual and decadal variations. The main study region is set in Myanmar (676,578 km^2). In the north, elevations are 20 m to 5000 m above sea level, while the highest mountain reaches over 5520 m (Figure 1(a)). Study analysis was carried out only during Myanmar's southwest summer monsoon season (MSwM); on the other hand, hazard risk analysis was carried out during Myanmar's peak rainfall

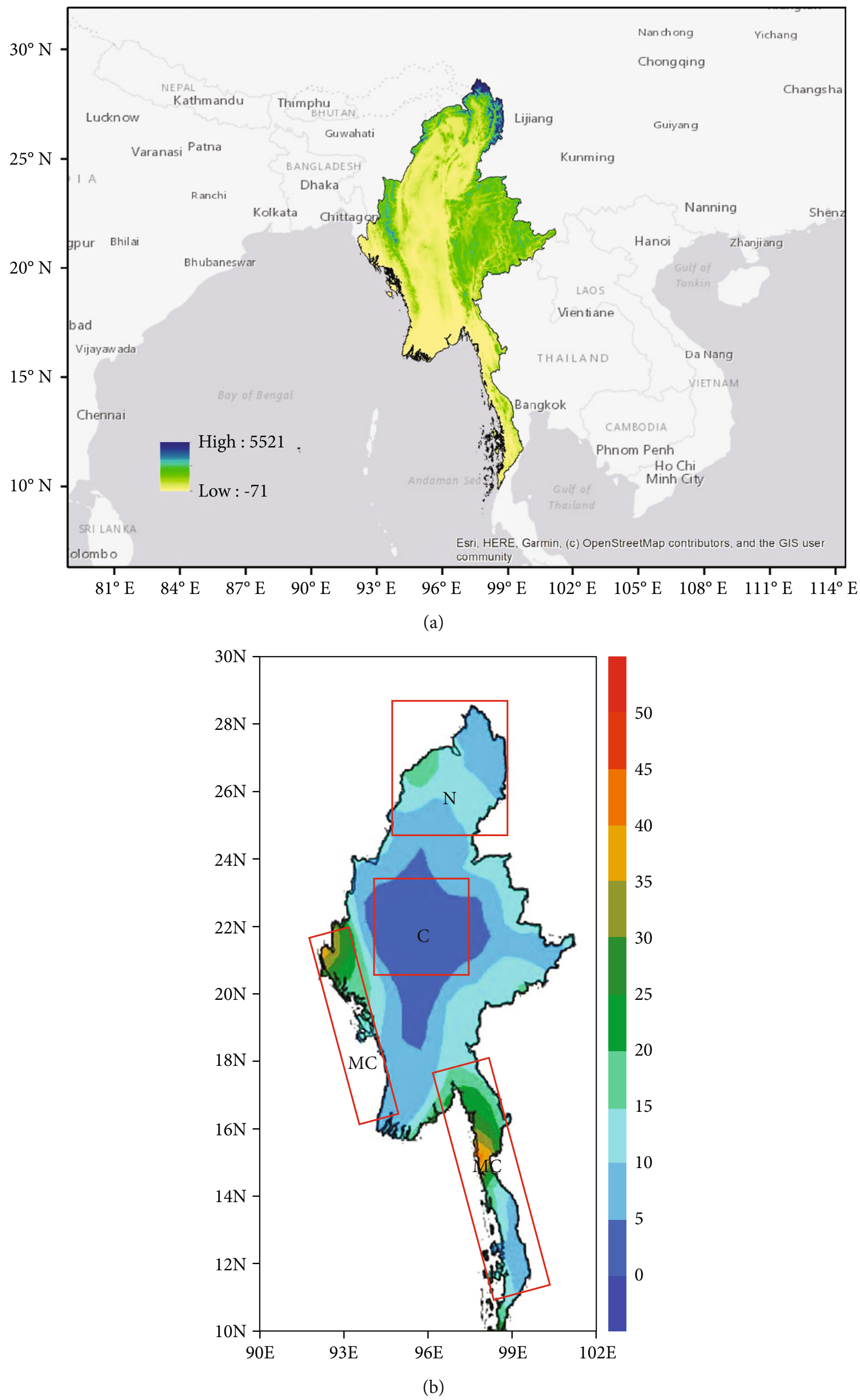

Figure 1: Study area (a) elevation (m) map and (b) spatial distribution of climatology maximum daily rainfall (mm) for southwest monsoon season during 1981-2020. The red boxes explain the homogeneous rainfall zone for the monsoon core (MC) region and central (C) and northern (N) Myanmar by the Htway and Matsumoto [6] and Oo [3].

season and peak flood and earthquake season by Myanmar Hazard Risk analysis [4]. The mean maximum daily rainfall is less than 5 mm per day in central Myanmar with around 50 mm per day in the northern, southern, and western coastal regions which are also known as monsoon core regions from 1981 to 2020 [3, 5].

In addition to these studies, several other studies have examined various aspects of monsoon rainfall in Myanmar, including its impact on agriculture, hydrology, and the environment. For example, a study by Thwe et al. [7] investigated the relationship between monsoon rainfall and rice production in Myanmar, while a study by Fritz et al. and Latrubesse et al. examined the impact of monsoon rainfall on river discharge and sediment transport in the Ayeyarwady River basin [8, 9]. Heavy rainfall over northern Myanmar is important for the country's agriculture industry and the Ayeyarwady River, and this relationship has been the subject of numerous studies in recent years [10]. The river basin is the home of a large number of people who depend on agriculture for their livelihoods. Moreover, the heavy rainfall also plays in maintaining the water levels at the Ayeyarwady River. The river also provides a cost-effective means of transport for goods such as rice, timber, and minerals [11]. However, heavy rainfall can also lead to flooding, which can cause damage to crops, infrastructure, and homes [12]. In recent years, Myanmar has gone through severe floods, which have displaced thousands of people and caused significant economic losses. Furthermore, earthquakes and heavy rainfall are generally not directly related to each other, but there are some indirect connections between the two phenomena [13]. Some studies have examined the relationship between rainfall and natural hazards in northern Myanmar [14, 15].

1.1. Hazard Analysis. Natural disasters present dangers to humans and their property [17]. Tropical cyclones with associated surges, floods, and drought are the most frequent natural disasters in Myanmar [18]. Climate change is expected to increase the frequency and severity of extreme weather events, such as prolonged periods of rain [19]. Rainfall that does occur will be more severe since the atmosphere is warmer and can contain more moisture [20]. This can result in increased flooding, landslides, and other related hazards. Figure 2 exhibits the frequency of natural hazards in Myanmar, and it can be found that earthquakes and floods are major hazards in weighted mode. Heavy rainfall over northern Myanmar is critical for the country's agriculture industry and the Ayeyarwady River [21]. While it provides vital water resources for irrigation and transportation, it can also lead to flooding and other challenges.

1.1.1. Earthquake. Earthquakes are brought on by the abrupt release of energy from tectonic plates in the Earth's crust [22]. Similarly, heavy rainfall can trigger landslides, which can, in turn, cause earthquakes. Although earthquakes and rainfall are two distinct natural occurrences, there are some similarities in the principles underlying both. Studies on earthquake prediction have exploited abnormalities in land surface temperature that have been seen before earthquakes [23]. Weather events have an impact on tectonics as well. Microseismic events can be caused by storms and typhoons [24], which can also be triggered by heavy rainfall [25]. This is because landslides can alter the stress on faults and cause them to slip, leading to seismic activity [26]. In addition, some research suggests that changes in the water table due to heavy rainfall can also contribute to earthquakes. The weight of heavy rainfall can also cause stress on the Earth's crust, which can trigger small earthquakes [27]. When the water table rises, it can increase the pore pressure in the Earth's crust, which can reduce the friction on faults and make them more likely to slip [28].

Moreover, studies using long time series of data have shown some evidence of local thermal and rainfall abnormalities before earthquakes. For example, most strong earthquakes in Southern California are preceded by a drought-flood pattern consisting of a few years of drought (below-normal rainfall) terminated by one or more consecutive seasons of heavy (above-normal) rainfall [30]. Kraft et al. [31] found that seismicity had a significant correlation with rainfall and groundwater levels. Overall, while earthquakes and heavy rainfall are not directly related, there are some complex and indirect connections between the two phenomena [32, 33]. The relationship between heavy rainfall over northern Myanmar and the Sagaing faults, which are the main trigger of earthquakes in the country, has been the subject of several studies [34–36]. Northern Myanmar is located also in a seismically active region and has experienced several earthquakes in the past [37]. A rising body of research examines the connection between rainfall and earthquakes in Myanmar, especially in the northern region.

Wang et al. [15] examined the impact of rainfall on seismicity regions including northern Myanmar. Zhang et al. [13] investigated the relationship between rainfall, landslides, and seismic activity using satellite and ground-based observations. The authors suggested that the observed correlation between rainfall and earthquakes was likely due to the effects of rainfall-induced pore pressure changes in the subsurface, which can trigger or facilitate the occurrence of earthquakes. Additionally, Figure 3 simulates that a large water load of five days accumulated heavy rainfall (~300 mm) that can suppress seismicity, while surface water is unevenly distributed (for example, water that is concentrated in a valley or on a mountain). However, their relationship still needs further study.

1.1.2. Floods. A flood is a natural phenomenon that arises from abnormal weather conditions, such as heavy rainfall, melting snow, coastal storms, and the failure of control works like dams [38]. It typically begins suddenly, grows rapidly, and spreads widely, causing significant damage to property and loss of life. Floods can quickly escalate into disasters when human settlements occupy flood-prone areas [39]. In Myanmar, floods occur mainly during the monsoon season from June to October [18]. These floods can generally be classified into two types: widespread floods that occur along major rivers like Ayeyarwady, Thanlwin, Chindwin,

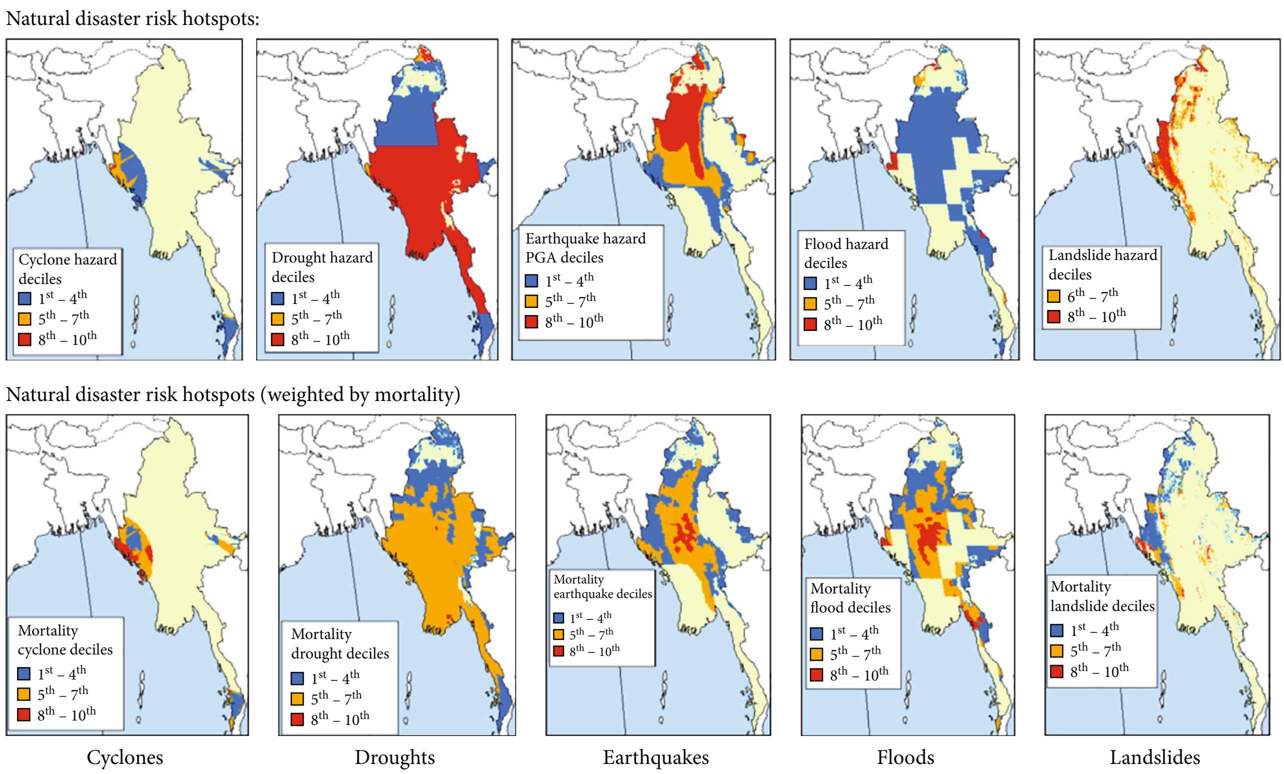

FIGURE 2: Spatial distribution (frequency) map of a natural disaster by major categories [16].

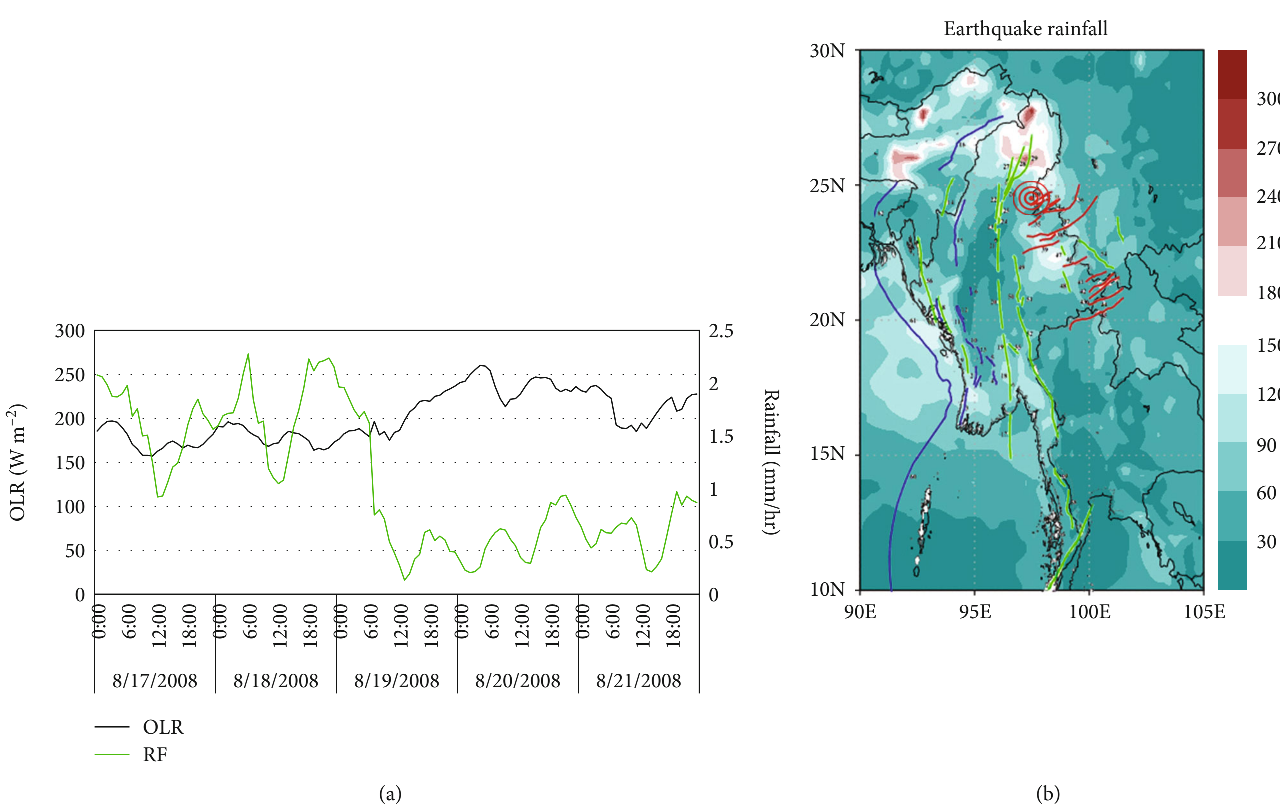

FIGURE 3: Composite simulated a significant earthquake (Richter 6.3) on 21 August 2008 (center location—red circles). (a) Hourly variation of rainfall (mm) amount and OLR value 5 days ahead of the event and (b) spatial 5-day total rainfall (mm) with overlay fault map by types, reverse (blue lines), right lateral (green lines), and left lateral (red lines), by Hlaing et al. [29].

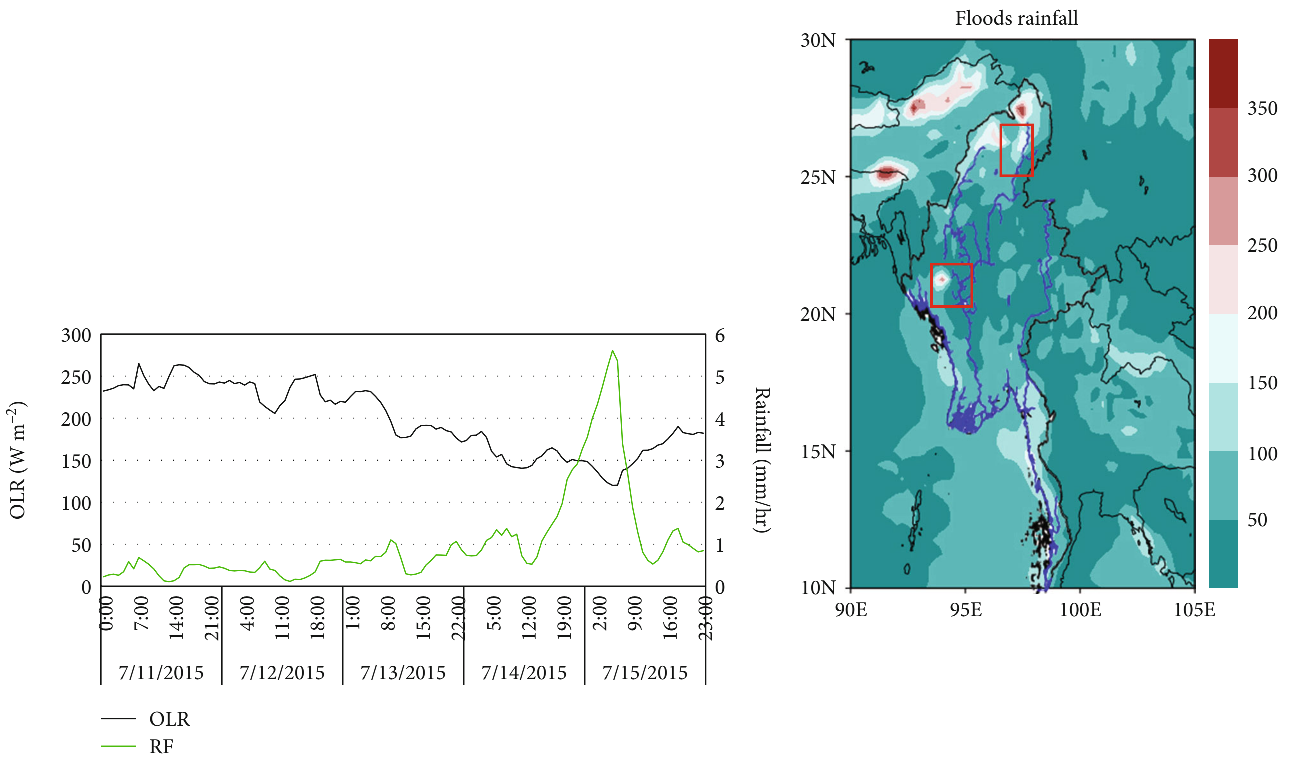

(a) (b)

Figure 4: Composite simulated a major flood on 11 July 2015 (flood area—red box). (a) Hourly variation of rainfall (mm) amount and OLR value 5 days ahead of the event and (b) spatial 5-day total rainfall (mm) shaded with major rivers (blue lines.

and Sittoung and flash floods that typically occur in small streams and rivers [40].

For instance, a study by Chhin et al. investigated the spatiotemporal distribution of rainfall and its impact on landslides in northern Myanmar between 2001 and 2017 [41]. The study found that landslides in the region were strongly associated with intense rainfall events, particularly during the southwest monsoon season. Another study [42] examined the effects of variable rainfall on riverbank erosion in the Ayeyarwady River. The study found that increased rainfall intensity and duration during the southwest monsoon season were the primary drivers of riverbank erosion in the region, particularly in areas with steep slopes and low vegetation cover. Additionally, several other researchers have looked into how rainfall affects natural disasters in northern Myanmar, such as flash floods and debris flows [43, 44].

According to observations, the occurrence of floods that exceed the level of risk in Myanmar's medium- and large-sized rivers is 6% in June, 23% in July, 49% in August, 14% in September, and 8% in October [45]. The most severe floods in Myanmar happened in 2004, 1974, 1997, 1976, 1991, 1973, 1988, and 1997. These years are arranged in order of their intensities. This severe flood event on 11 July 2015 by extremely heavy rainfall is simulated in Figure 4.

The region's rainfall phenomena and river flow are related; therefore, it makes sense to analyze several factors at once to acquire a total understanding. Therefore, using observation data and predicted outputs from five GCMs (global circulation models) from CMIP6 (Coupled Model Intercomparison Project from Phase 6), the specific goal of the current study is to explore changes in past and future extremes of rainfall over the Ayeyarwady River basin. The CMIP6 model simulates two SSP (2-4.5 and 5-8.5) scenarios and assesses how much the climate has changed after 80 years [46].

In terms of projections for northern Myanmar specifically, regional model downscaling from the Weather Research and Forecasting (WRF) model that is developed by the Department of Meteorology and Hydrology suggests that heavy rainfall events will become more frequent and intense in the future [47, 48]. This can have significant impacts on the region's water resources, agriculture, and infrastructure. To mitigate the impacts of heavy rainfall, the government of Myanmar has implemented various measures, including the construction of dams and reservoirs, the development of early warning systems, and the provision of flood relief and recovery assistance. Following are the remaining details of this study outline: the brief explanation of the study region, data used, and the method of downscaling GCM outputs and calculation of climate extreme indices and intensity-duration-frequency (IDF) curves are described in Section 2. Results are presented and discussed in Section 3, and the study's conclusion is discussed in Section 4.

2. Data and Method

2.1. Observation Data. To investigate the significant level of ECMWF Reanalysis v5 (ERA5) data [49] with rain gauge

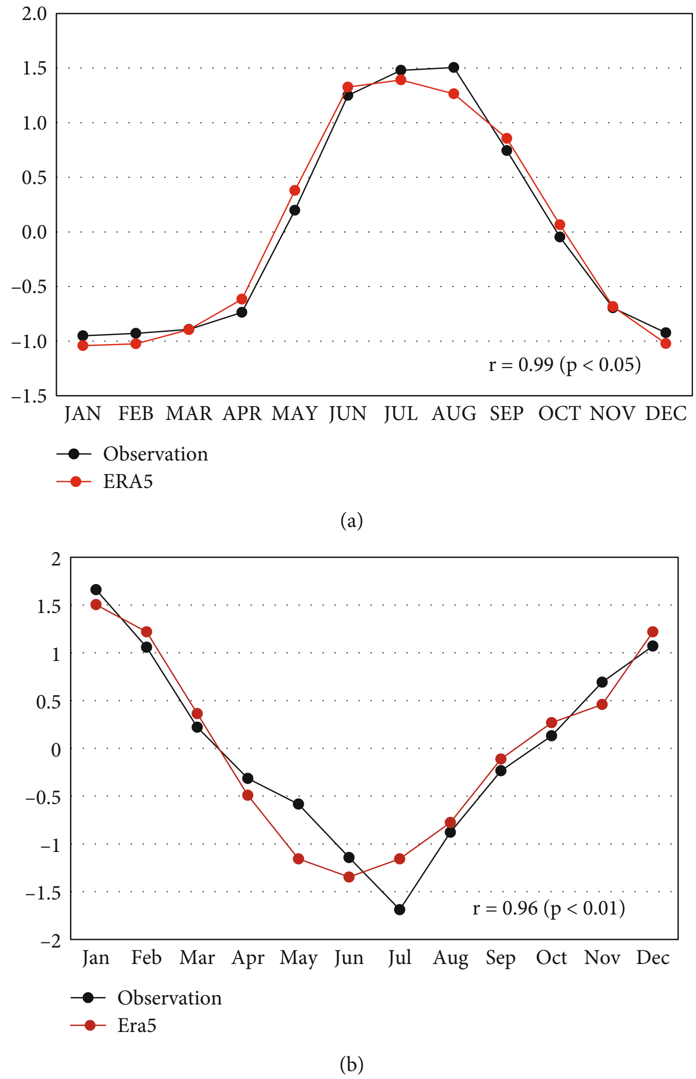

Figure 5: The mean annual cycles of normalized rainfall from ERA5 and observed stations. (a) Monthly rainfall and (b) mean sea level pressure, averaged over longitudes 92°E to 103°E and latitudes 10°N to 30°N over the period 1991-2020 [3].

observation data, the statistical downscale correlation test was performed. ERA5 has high intraseasonal correlations with 79 observation station data with 90% significant level (Figure 5). The temporal resolution of the study is from 1981 to 2020 for climatology and 2021 to 2099 for future projection and only focuses on major rainfall season (JJA) (well-known as "global summer"), due to the high hazard frequency distribution [50, 51].

2.2. Intensity-Duration-Frequency (IDF) Curves. Typically, IDF curves are constructed to estimate return periods by combining a series of observed rainfall data with the desired rainfall duration's distribution type [52–54].

Theoretical distributions including the Gumbel, log-normal, and log-Pearson type III distributions have been used in various applications in different parts of the science research [54, 55]. The Gumbel, log-normal, and log-Pearson type III distributions—commonly employed frequency analysis techniques—were used to conduct the analyses for return periods of 2, 5, 10, 50, and 100 years [56].

All observed rainfall data must be converted into mm/hr units because intensity-duration-frequency (IDF) curves are created using a technique in which intensities are measured in mm/hr and durations are measured on a horizontal axis (Eq. (1)). Consequently, the method below is used to calculate intensities in terms of millimeters per hour [57, 58].

$$i = \frac{R}{T_{\mathrm{D}}}, \tag{1}$$

where R is the rainfall depth in mm and T_{D} is the rainfall duration in hours.

2.2.1. Gumbel Distribution. Gumbel [56] presented the theory of extremes by considering the distribution of the largest or the smallest values observed in repeated samples. The Gumbel theory is the most widely used distribution for IDF analysis due to its suitableness for modeling maximum data. It is relatively easy and it can be used only for extreme

Table 1: Gumbel distribution.

(a)

	1 hr	3 hr	6 hr	12 hr	24 hr
Mean	13.41071	11.53311	9.502405	6.586385	4.516272
St. dev.	1.313377	1.291345	1.096353	0.958661	0.779865

(b)

Frequency factor K_T return	2 years	5 years	10 years	50 years	100 years
	-0.164	0.719	1.305	2.592	3.137

(c)

Hour	2 years	5 years	10 years	50 years	100 years
1	13.20	14.36	15.12	16.81	17.53
3	11.32	12.46	13.22	14.88	15.58
6	9.32	10.29	10.93	12.34	12.94
12	6.43	7.28	7.84	9.07	9.59
24	4.39	5.08	5.53	6.54	6.96

The calculated K_T values which are utilized in analyses, the rainfall amounts with respect to specific durations, and the return periods for log distribution.

Table 2: Log-Pearson type III distribution.

(a)

	1 hr	3 hr	6 hr	12 hr	24 hr
Mean	13.41071	11.53311	9.502405	6.586385	4.516272
St. dev.	1.313377	1.291345	1.096353	0.958661	0.779865

(b)

Frequency factor K_T return	2 years	5 years	10 years	50 years	100 years
	0.116	0.857	1.183	1.663	1.806

(c)

Hour	2 years	5 years	10 years	50 years	100 years
1	13.56	14.54	14.96	15.59	15.78
3	11.68	12.64	13.06	13.68	13.87
6	9.63	10.44	10.80	11.33	11.48
12	6.70	7.41	7.72	8.18	8.32
24	4.61	5.18	5.44	5.81	5.92

The calculated K_T values which are utilized in analyses, the rainfall amounts with respect to specific durations, and the return periods for log distribution.

events (maximum data or peak rainfalls) [59]. The design rainfall depth for a given period can be calculated by the following equation [57].

$$X_T = \overline{X_{T_D}} + K_T S_{T_D}, \tag{2}$$

where "S" show the mean and the standard deviation of different specified rainfall durations of T_D, respectively, and K_T is the frequency factor which can be calculated from the following formula.

$$K_T = -\frac{\sqrt{6}}{\pi}\left[0.5772 + \ln\left(\text{In}\ \frac{T}{T-1}\right)\right], \tag{3}$$

where T is the return period.

Table 3: Log-Pearson normal distribution.

(a)

	1 hr	3 hr	6 hr	12 hr	24 hr
Mean	13.41071	11.53311	9.502405	6.586385	4.516272
St. dev.	1.313377	1.291345	1.096353	0.958661	0.779865

(b)

Frequency factor K_T return	2 years	5 years	10 years	50 years	100 years
	0	0.842	1.282	2.054	2.326

(c)

Hour	2 years	5 years	10 years	50 years	100 years
1	13.41	14.52	15.09	16.11	16.47
3	11.53	12.62	13.19	14.19	14.54
6	9.50	10.43	10.91	11.75	12.05
12	6.59	7.39	7.82	8.56	8.82
24	4.52	5.17	5.52	6.12	6.33

The calculated K_T values which are utilized in analyses, the rainfall amounts with respect to specific durations, and the return periods for log distribution.

Table 4: Description of 5 GCMs from CMIP6 used in this study.

Model	Institution	Resolution	Grid (Lon × Lat)
ACCESS-CM2	Commonwealth Scientific and Industrial Research Organization-Australian Research Council Centre of Excellence for Climate System Science, Australia	$1.875^\circ \times 1.250^\circ$	16×16
CNRM-CM6-1	Center National de Recherches Météorologiques–Center Européen de Recherche et de Formation Avancée en Calcul Scientifique, France	1.5×1.5	22×14
EC-Earth3-AerChem	EC-EARTH consortium, the Netherlands/Ireland	$1.125^\circ \times 1.125^\circ$	43×29
FGOALS-g3	Chinese Academy of Sciences, China	$2.00^\circ \times 2.25^\circ$	16×10
MRI-ESM2-0	Meteorological Research Institute, Japan	$1.125^\circ \times 1.125^\circ$	27×18

Table 5: List of extreme precipitation indices by Expert Team on Climate Change Detection and Indices (ETCCDI) from the World Climate Research Program (WCRP).

ID	Index name	Definition	Units
R95p	Very wet days	Annual total precipitation when daily precipitation amount on a wet day >95th percentile	mm
RX1day mm	Max 1-day precipitation amount	Monthly maximum 1-day precipitation	mm
RX5day	Max 5-day precipitation amount	Monthly maximum consecutive 5-day precipitation	mm
R10	Number of heavy precipitation days	Annual count of days when precipitation ≥ 10 mm/day	days
R20	Number of very heavy precipitation days	Annual count of days when precipitation ≥ 20 mm/day	days

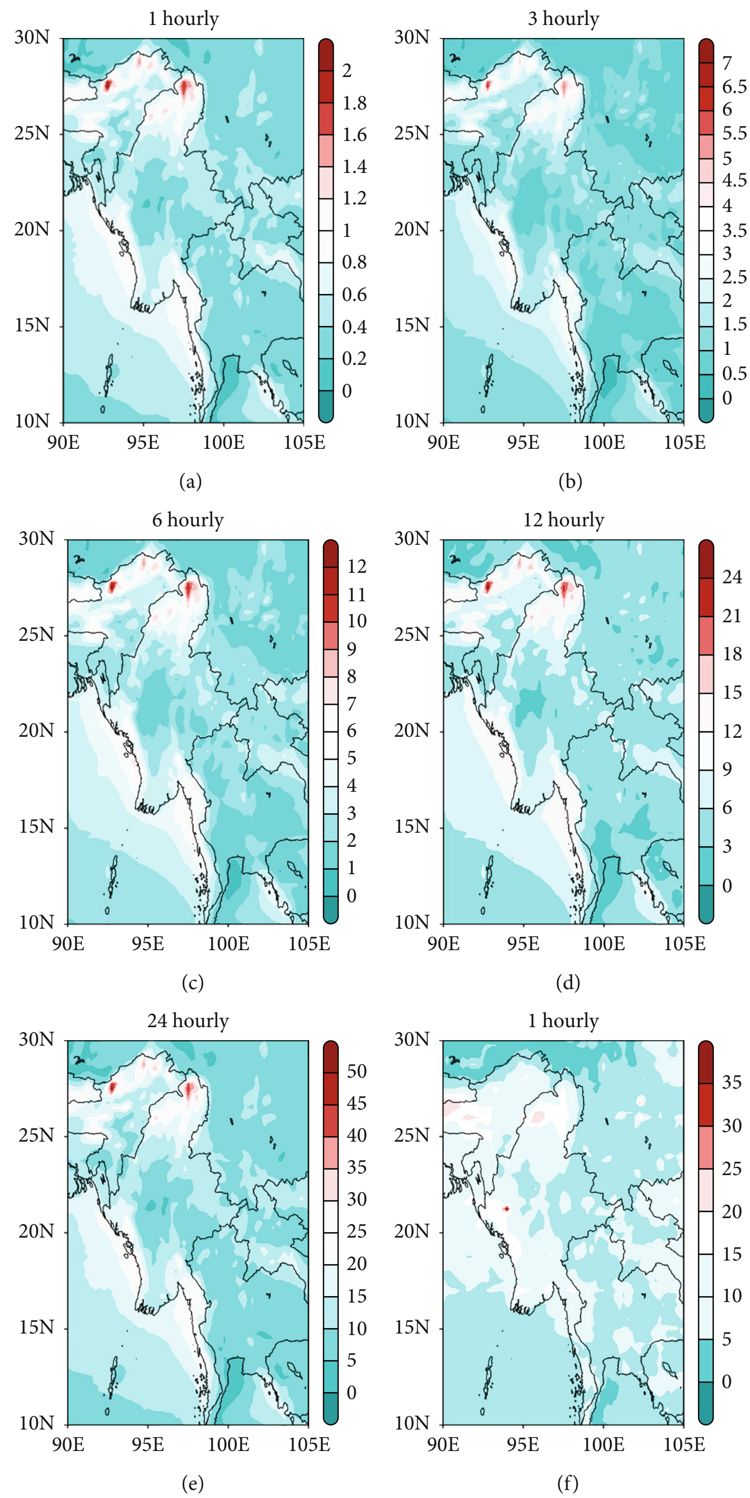

Figure 6: Continued.

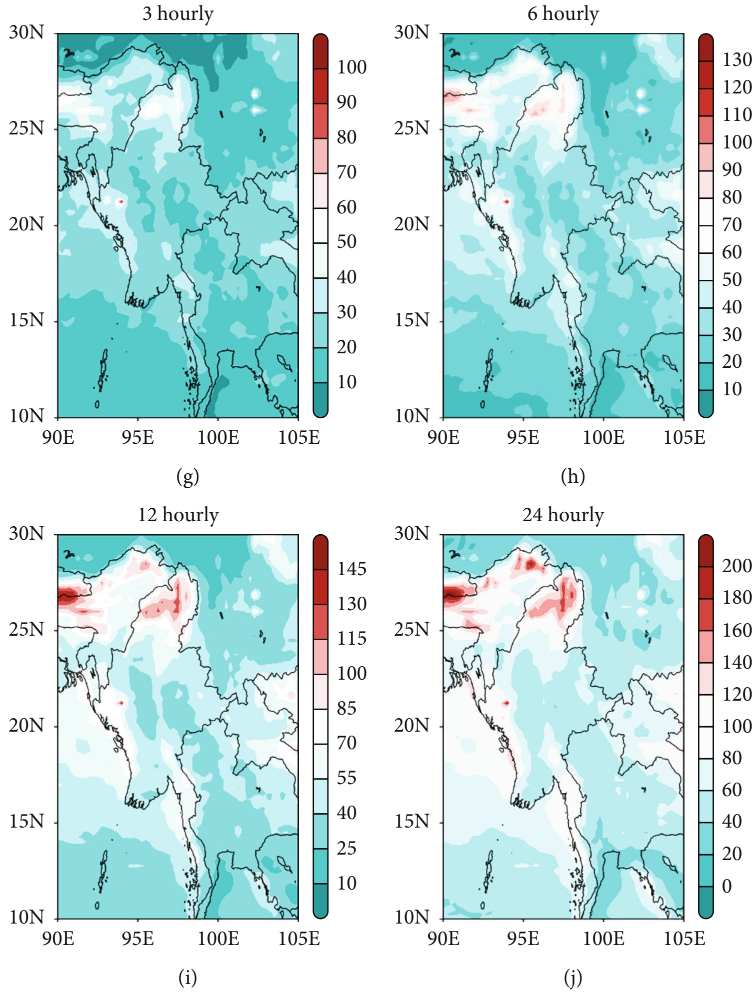

Figure 6: Composite climatology mean and maximum rainfall (mm) amount of (a, f) 1 hour, (b, g) 3 hours, (c, h) 6 hours, (d, i) 12 hours, and (e, j) 24 hours during 1981-2020.

2.2.2. Log-Pearson Type III Distribution. The log-Pearson type III distribution model is used to determine the rainfall intensity at different rainfall durations and return periods for generating the historical IDF curves. The log-Pearson type III distribution is frequently used for flood analysis. In this distribution, the following parameters of distribution must be calculated.

$$\overline{\log X} = \frac{\sum \log X}{n}, \tag{4}$$

where n is the number of data. Thus, magnitudes corresponding to a return period can be calculated by following the formula.

$$\log X = \overline{\log X} + K_T S_{\log X}. \tag{5}$$

The calculated K_T values which are utilized in analyses, the rainfall amounts concerning specific durations, and the return periods for log distribution are exhibited in Tables 1–3. The log-normal method also uses the same procedure of log-Pearson type III (i.e., logarithm values of the statistical variables) but with normal K_T (i.e., K_T used by the Gumbel method).

2.2.3. General Climate Model Simulation. The Copernicus 75 database provides publicly available global climate model (GCM) simulations for both historical and future periods [60]. Future projections are obtained using the emission scenarios "Shared Socioeconomic Pathway" 2-4.5 (SSP2-4.5) and 5-8.5 (SSP5-8.5), which are considered by the Scenario Model Intercomparison Project (Scenario MIP) of CMIP6 [61]. The study used an ensemble simulation from five GCMs, selected based on their availability under r1i1p1f1 initial conditions and the quality of their performance in simulating rainfall in the study region (Table 4 shows detailed information for 5 models). All the models providing future simulations for the two considered emission scenarios (SSP2-4.5 and SSP5-8.5) were selected. The historical period is defined as 1981-2020 since GCM simulations start from 1850. The models are gridded to observation datasets of $0.5^{\circ} \times 0.5^{\circ}$ using bilinear interpolation by using Climate Data Operator (CDO, version 2.0.4). The study uses the

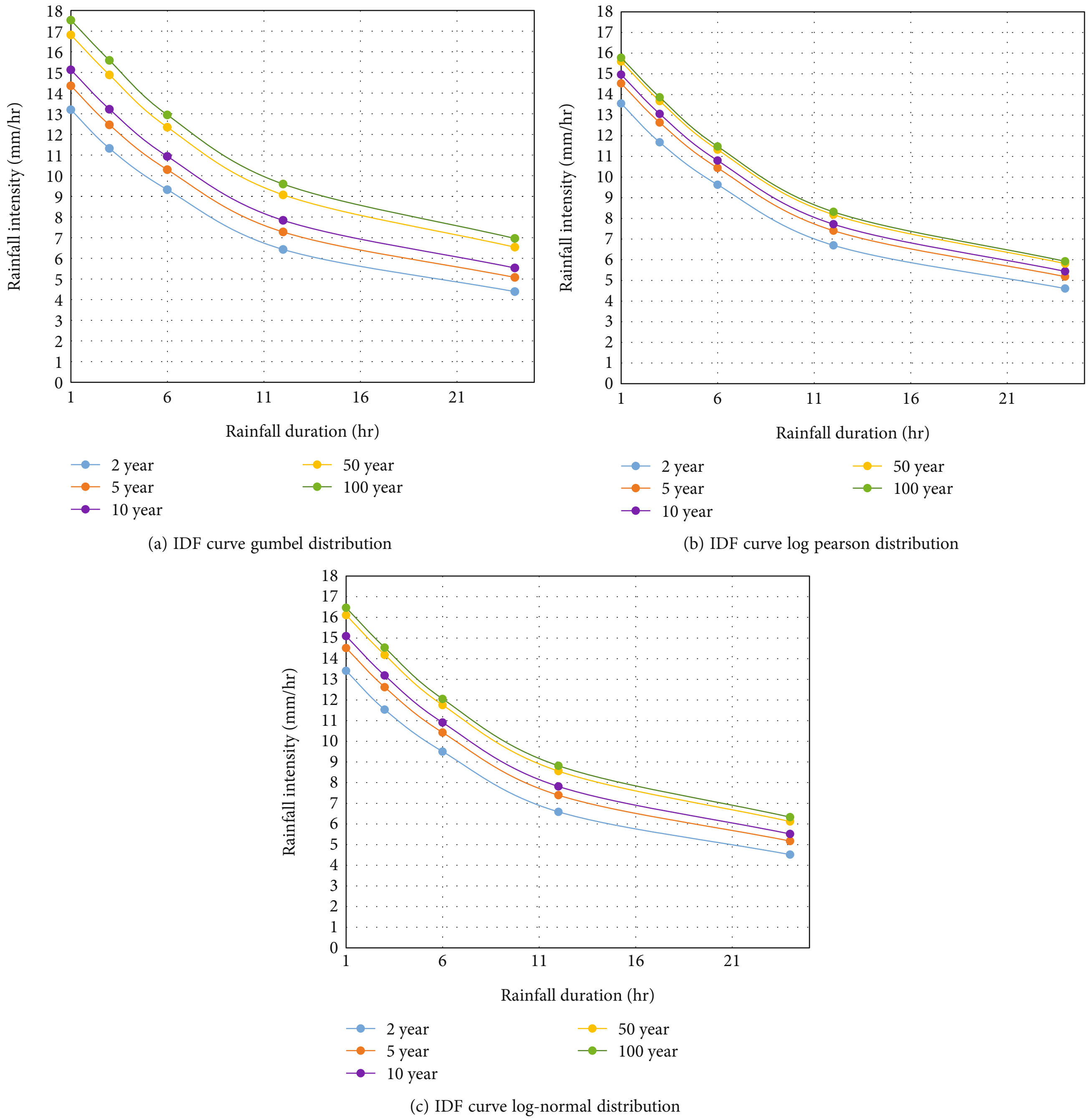

(a) IDF curve gumbel distribution

(b) IDF curve log pearson distribution

(c) IDF curve log-normal distribution

Figure 7: Intensity-duration-frequency (IDF) curves by different methods.

multimodel ensemble mean (MME) of the 5 GCM outputs (Equation (6)) for analysis, as MME is considered superior to individual models [62]. To compare the simulation with observed data, bilinear spatial interpolation is applied to estimate the model prediction.

We also aggregated the hourly datasets into daily and seasonal values using CDO. The climatology was quantified over the Mainland Indochina continent and the Bay of Bengal (BoB) by spatial and temporal averaging of the long-term dataset from 1981 to 2020. Both the CMIP6 GCMs and the reanalysis rainfall data (ERA5) reported the mean geographical bias. Based on Equation (6), the GCM ensemble mean (ESM) was calculated by averaging five different GCMs.

$$\mathrm{ESM} = \frac{1}{n}\sum_{i=1}^{n} \mathrm{GCMsi}. \tag{6}$$

To study the changes in climatic extremes, the Expert Team on Climate Change Detection and Indices (ETCCDI) created a core set of 27 indices [63]. The “Rclimdex”

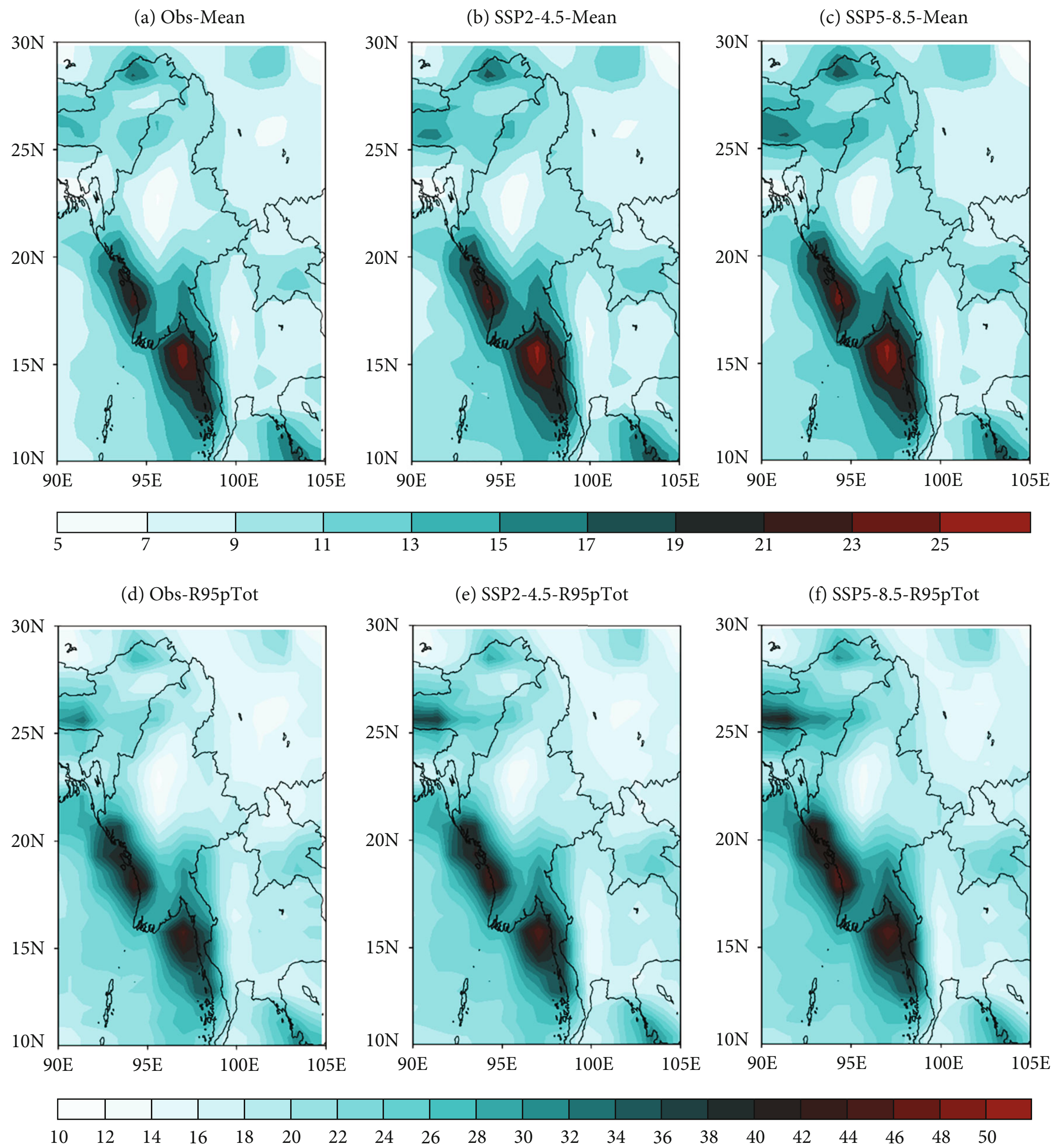

Figure 8: Simulated JJAS mean and extreme rainfall (mm). Spatial pattern of mean rainfall (Pr) (above) and very wet days (R95pTOT) (below) for (a, d) observation reanalysis during the period 1981–2020 and the multimodel ensemble mean of (b, e) SSP2-4 and (c, f) SSP5-8 during 2020-2100.

package is used to calculate the extreme indices [64]. To examine how the Ayeyarwady River basin's climate extremes have changed for this study, 5 rainfall indices were chosen. We evaluated the climatic extremes using the observed dataset (1981-2020) and future dataset (2021-2100) to comprehend how extreme rainfall evolved during the previous 30 years and to more precisely forecast how it will change in the following 30 years. The Pearson correlation and two-tailed t-test are mainly used for correlation analysis [65].

The spatial distribution of the mean JJAS rainfall, very wet day rainfall (R95pTOT), heavy rainfall day index per period (r10mm), very heavy rainfall day index per period (r20mm), maximum consecutive 1-day rainfall (RX1day), and maximum consecutive 5-day rainfall (RX5day) is explained in the next section. The detailed calculation method and definitions of indices are explained in Table 5.

3. Result and Discussion

Before finding the projection of maximum rainfall amount and intensity, climatology maximum rainfall amount by 5 periods (1, 3, 6, 12, and 24 hours) are carried out. The spatial composite climatology rainfall intensity of the above 5 periods is shown in Figures 6(a)–6(e). The northern and monsoon core regions show high intensity in each period

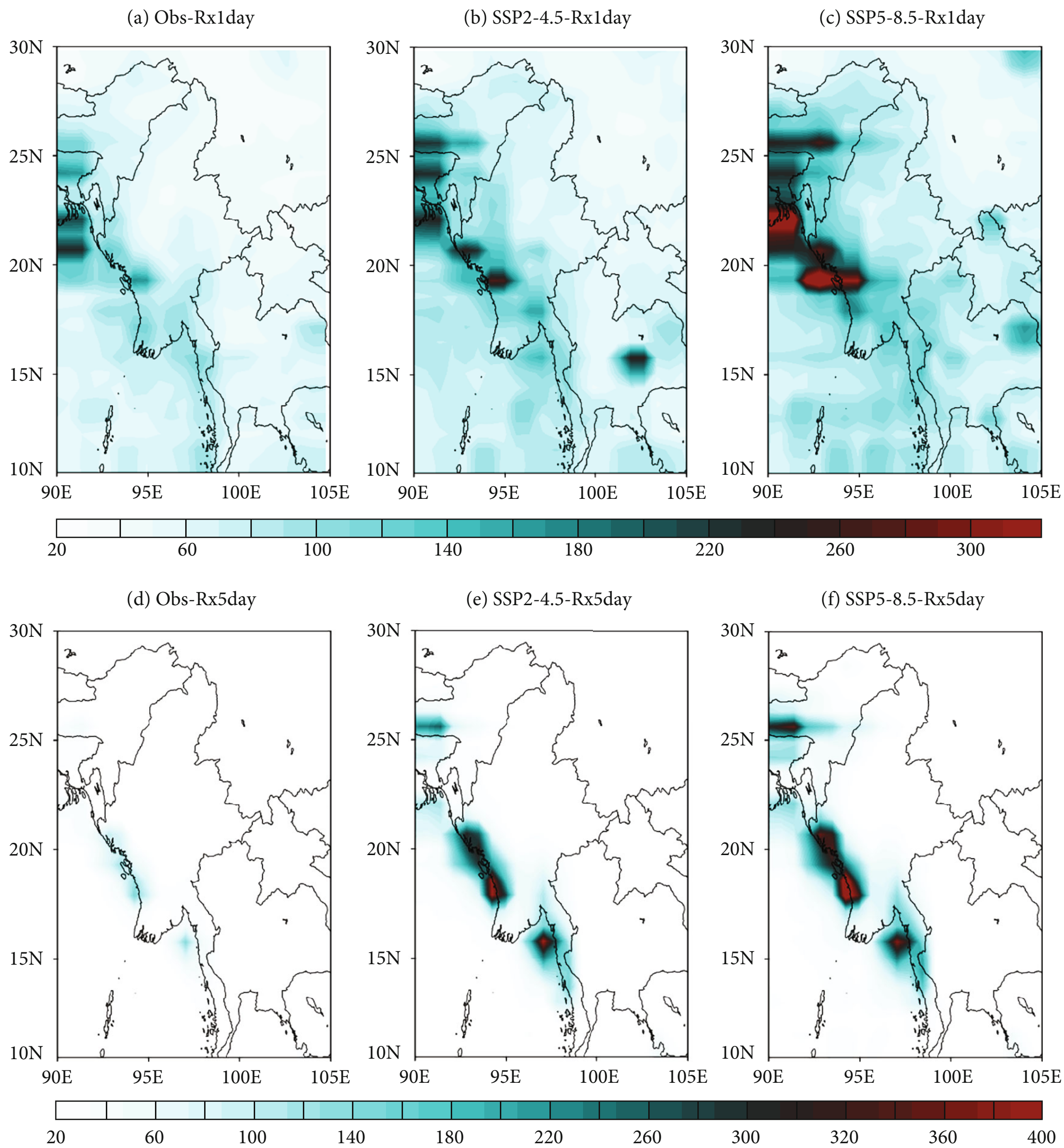

Figure 9: Simulated mean rainfall and extreme rainfall (mm). Spatial pattern of maximum 1-day rainfall (RX1day) (above) and maximum consecutive 5-day rainfall (RX5day) (below) for (a, d) observation reanalysis during the period 1981–2020 and the multimodel ensemble mean of (b, e) SSP2-4 and (c, f) SSP5-8 during 2020-2100.

from 1981 to 2020. The central region shows less intensity, which agrees with the previous studies [66, 67]. The maximum values for the same period are also exhibited in Figures 6(f)–6(j). The amount of 35 mm to 200 mm of rainfall is found in the same region during the study period. It means the northern Himalaya foothill region and MSwM core regions are the dominant areas for high rainfall intensity during the summer monsoon season. Both analyses agree with each other. Furthermore, we take only three regions for further analysis: northern Myanmar, the Eastern Himalaya foothill region, and the monsoon core regions. Additionally, Sun et al. [55] explained the calculation process and approach that the intensity-duration-frequency (IDF) curve is the best tool to determine the accurate result of rainfall intensity with time. This region is also the highest natural disaster region as mentioned in the previous section.

Intensity-duration-frequency (IDF) curves for major risk zones (92°E-98°E-26°N-28°N) are calculated using both ERA5 and GCM data to characterize the variance and relationship between rainfall intensity, rainfall duration, and return time over the study area. This hydrologic and water resource system design frequently employs IDF curves. By analyzing the frequency of rainfall readings, IDF curves are produced. Additionally, Sun et al. [55] explained the calculation process and approach, and intensity-duration-

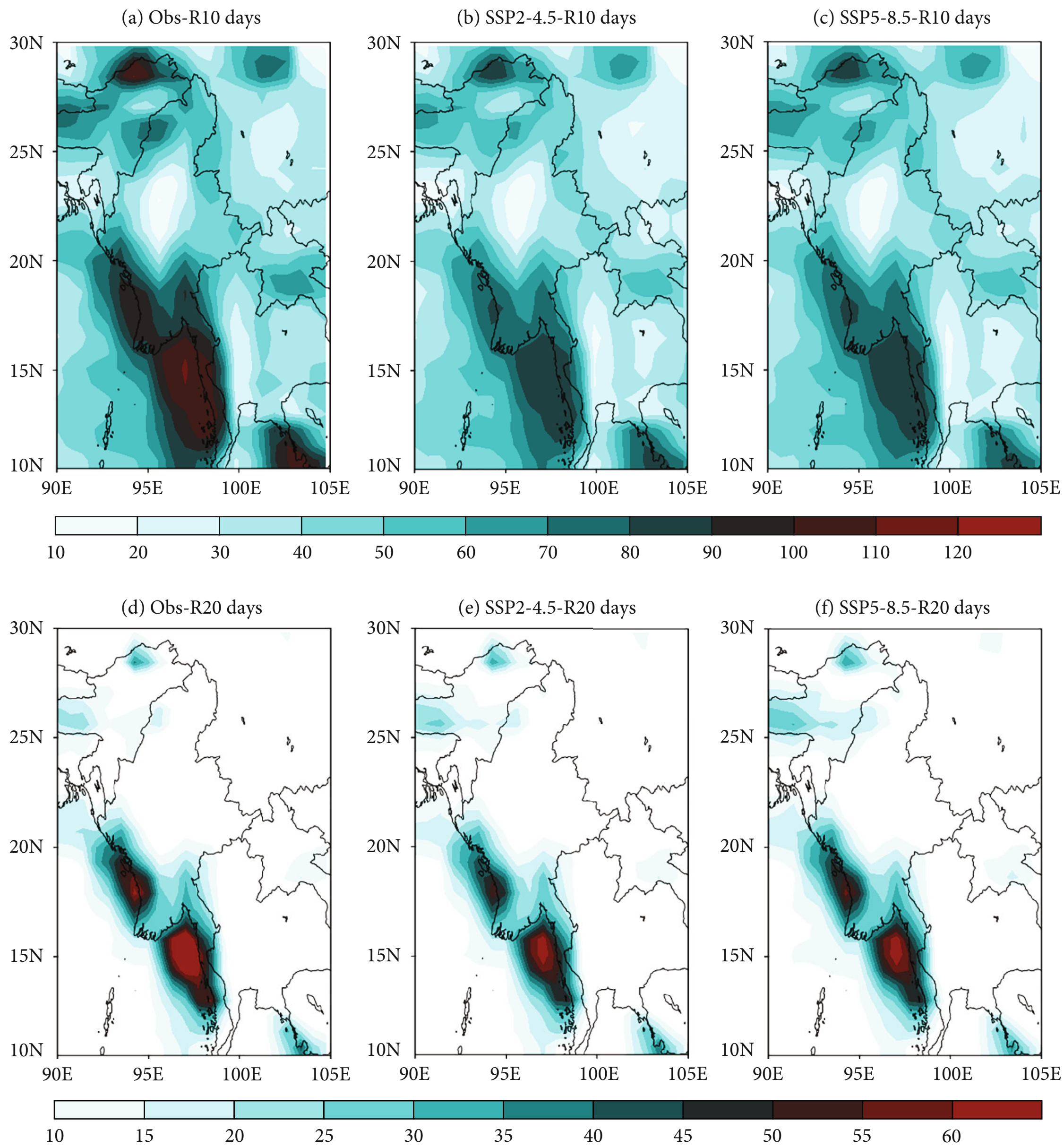

Figure 10: Simulated mean rainfall and extreme rainfall (days). Spatial pattern of annual count days when rainfall ≥ 10 mm (R10mm) (above) and annual count days when rainfall ≥ 20 mm (R20mm) (below) for (a, d) observation reanalysis during the period 1981–2020 and the multimodel ensemble mean of (b, e) SSP2-4 and (c, f) SSP5-8 during 2020-2100.

frequency (IDF) curve is the best tool to determine the accurate result of rainfall intensity with time. Intensity-duration frequency (IDF) curves, which are derived from several analyses of observed rainfall data, show a link between rainfall duration, intensity, and frequency (return period). The 40 years of rainfall data, from 1981 to 2020, was used to determine the yearly maximum rainfall depths for the particular times. The focus of this analysis is to outcome IDF curves for the northern Myanmar region for each rainfall period of 1 hr, 3 hr, 6 hr, 12 hr, and 24 hr. For return periods of 2, 5, 10, 50, and 100 years, analyses using the widely used frequency analysis techniques Gumbel, log-normal, and log-Pearson type III distributions were carried out. For every duration with a certain return period (years), rainfall frequency (mm) can be determined. After that, the intensity of rainfall (in mm/hr) for each return period is exhibited as shown in Figure 7. The findings showed that as the short duration lengthens, rainfall intensity increases. As opposed to that, the much rainfall amount in short duration pattern is dominant for the future. Additionally, when there is a long return period, rainfall with a specific length has a higher intensity.

The results of this investigation are anticipated to be helpful to the local authorities of the region. It is possible to estimate floods in both rural and urban basins using the IDF curves. The IDF's generated curves should be used to

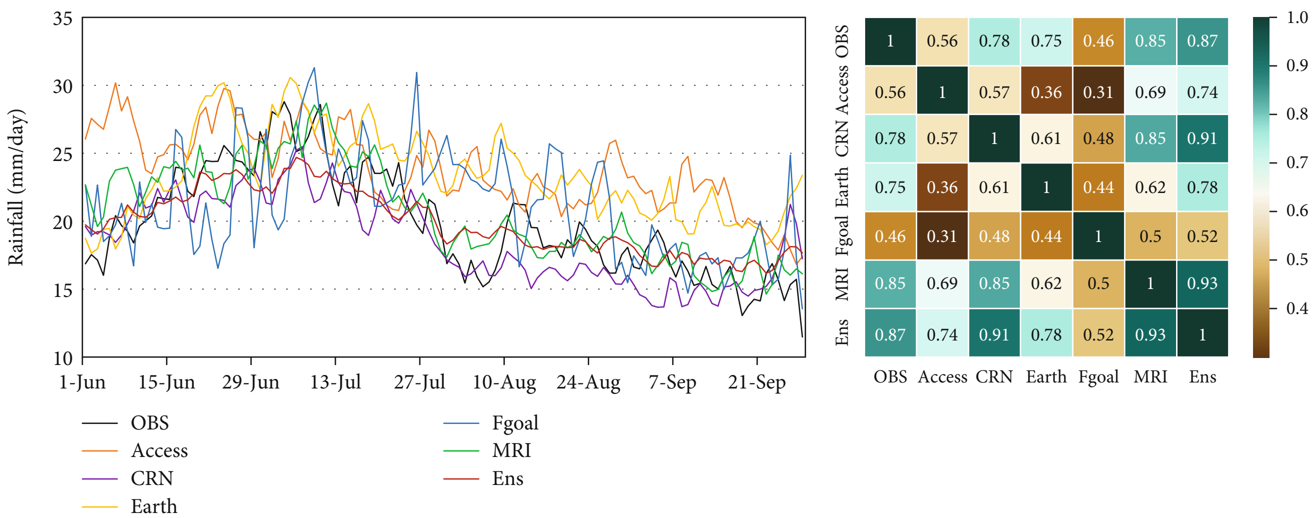

(a) (b)

Figure 11: Climatology of historical (1981-2014) mean daily rainfall (mm/day) of Ens-Model (MME) and CMIP6 models against observation data (a) with their correlation heatmap (b).

Table 6: The seasonal correlation significant values of mean daily rainfall (mm/day) of MME and CMIP6 models against observation data.

	Access	CRN	Earth	FGoal	MRI	Ens-MME
OBS	0.56**	0.78**	0.75**	0.46**	0.85**	0.87**

**Correlation is significant at the 99% (0.001) level (2-tailed).

safely, effectively, and scientifically construct flood protection projects. The generated IDF curves can then be used, as seen in Figure 7.

The regional spatial distribution of the mean rainfall and the very wet day rainfall (R95pTOT) for the ensemble mean of two GCM scenarios and the observation data are shown in Figure 8. According to the ERA5 reanalysis, the average daily rainfall recorded for the years 1981 to 2020 is higher in northern Myanmar (above 25 mm) than in the monsoon core region (25 mm) and remainder of the area (below 10 mm) (Figure 8(a)). The eastern edge of India and central regions of Myanmar experienced total rainfall records at a long-term average of 95 percentile (up to 40 mm) (Figure 8(d)). The simulations show that the summer JJAS mean rainfall of the northern Myanmar region has changed dramatically, while the western and southern coastal (monsoon core) areas of Myanmar have experienced less change by two scenarios of the GCMs.

The maximum 1-day rainfall amount (RX1day) showed a markedly declining trend (Figures 9(a)–9(c)) with an annual magnitude of >100 mm over northern Myanmar and >200 mm over southern coastal Myanmar. However, the western coastal region has less change for the three scenario phases. Between 50 and 200 mm were the ranges for the basin average RX1day for the 1981–2020 baseline period. Additionally, variations between 50 and 200 mm of the maximum 5-day rainfall show a similar trend. It shows that the heavy rainfall events occurred in a short time for this area. Under SSP scenarios, the expected rises and decreases have larger magnitudes, possibly because of the higher forcing.

Overall, the future rise in the summer southwest monsoon's rainfall variability across mainland Indochina is linked to more wet days in a row and more intense downpours, and it could have significant effects on the region's water resources, agriculture, hydroelectric power production, and social stability. However, in the extreme day analysis for the same period, there were between 10 and 100 days with heavy rainfall (R10 days). At the 95 percent confidence level, the number of days with heavy rain decreased by 0.5 days per year in the monsoon core region and 0.2 days per year in the northern Myanmar region (Figure 10). Nevertheless, reverse patterns are clear over northern regions for three scenarios in very heavy rainfall day (R20) analysis and the slight change found over monsoon core regions with a variation of 10 to 30 days for western coastal regions and 5 to 10 days for southern coastal regions. In summary, this can be assumed that very heavy rainfall intensity in short duration is more strong and dominant in future climate change.

3.1. Future Changes

3.1.1. Evaluation of Simulated Mean and Extreme Rainfall. Before the projection of the future climate change impact on MSwM rainfall variability by the GCMs, we performed the correlation test of the models' data and observation data. To assess how well the observed and GCM simulations agreed, the climatological rainfall patterns were computed. We averaged the daily values at each grid point to obtain the spatial climatological mean into yearly and seasonal categories. Figure 11 and Table 6 explain the seasonal correlation significant values of mean daily rainfall (mm/day) of observation, MME, and CMIP6 models. The high positive correlation between observation data and GCMs is found at a 99% confidence level by the Pearson correlation test.

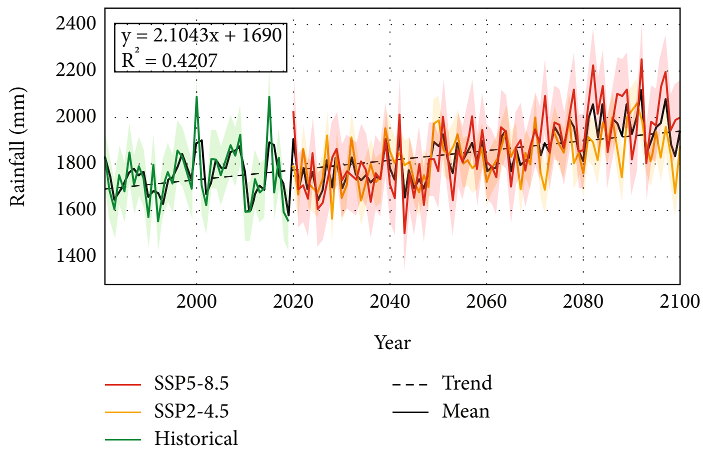

(a)

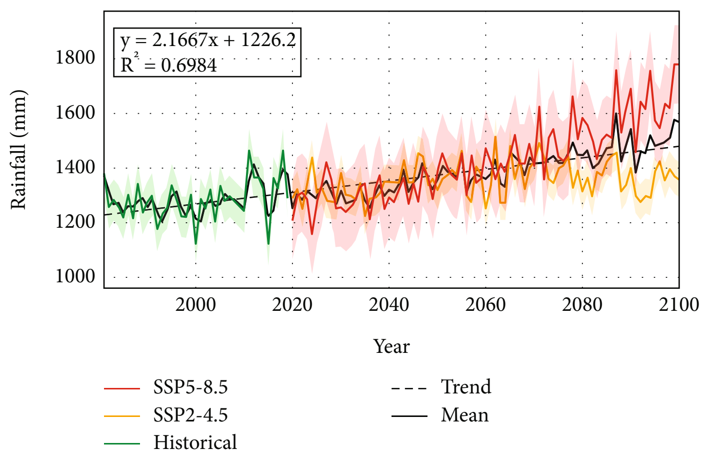

(b)

Figure 12: Annual rainfall time series for both historical period simulation and future projections (mm/year). Historical (green), climatology mean (black), and future MME simulations for SSP2-4.5 (orange) and SSP5-8.5 (red). And dotted line shows the linear trend of each for (a) the monsoon core region and (b) the northern regions (linear regression R^2 value, orange box for SSP2-4.5 and red box for SSP5-8.5).

3.1.2. Changes in Average Rainfall. The future projections (2021-2099) of annual extreme rainfall for two different scenarios (SSP2-4.5 and SSP5-8.5) were compared with the MME simulation of the historical period (1981-2020) by time series simulation in Figure 12. Future annual rainfall shows the significant increase for the SSP5-8.5 scenario with the slight increase for the SSP2-4.5 for both regions. To inspect the temporal progress of changes, the annual cycle of rainfall is considered and the future period is divided into near future (2021-2060) and long future (2061-2099) related to the present-day simulation (1981-2020). While the fluctuation of the first decades was close to stationary variability concerning the historical period, the long future has a high fluctuation range, especially for SSP5-8.5. This analysis outcome agrees with the suggestion of previous climate change studies and report by IPCC [68, 69].

4. Summary and Discussion

Based on the potential influence of climate change on daily rainfall patterns, the study explores the characteristics and variability of monsoon rainfall in Myanmar, with a discussion of the relationship between heavy rainfall, floods, and earthquakes in Myanmar, which influence agriculture, hydrology, and the environment. Myanmar's rice cultivation relies on monsoon rainfall, ensuring irrigation resources and maintaining water levels in the Ayeyarwady River basin. However, heavy rainfall can cause flooding, economic losses, and water table changes. The two scenarios of CMIP6 models predict increased intensity and frequency of heavy rainfall events, impacting water resources, agriculture, and infrastructure. Based on the above preliminary analysis, the following major results are out of this study.

(1) The GCM simulations for both historical and future projections of two emission scenarios SSP 2-4.5 and 5-8.5 explain that northern Myanmar, the eastern Himalaya foothill region, and MSwM core regions are the dominant areas for high rainfall intensity area rather than the others during the summer monsoon season

(2) Further analysis examines climatology, and rainfall intensity for five periods (1, 3, 6, 12, and 24 hours) results that high intensity has been found over the northern region and monsoon core regions with the maximum values ranging from 35 mm to 200 mm, while the central region shows less intensity during summer moons

(3) Intensity-duration-frequency (IDF) curves explain that as high rainfall intensity in short duration lengthens, future rainfall patterns increase in all three return years time over major risk zones

(4) The spatial rainfall distribution of average rainfall and very wet day rainfall for two climate change scenarios by the observation data shows a significant change in rainfall in northern Myanmar and less change in the monsoon core regions from 1981 to 2020. This exceed in extreme rainfall variability is linked to more wet days and intense downpours, potentially impacting water resources, hydroelectric power production, agriculture, and social stability

(5) The maximum 1-day rainfall in northern and southern Myanmar shows a declining trend, with annual magnitudes of around 150 mm and 100 mm, respectively. With the range of 50 and 300 mm, the maximum 5-day rainfall shows a reversed trend over the northern region

In conclusion, Myanmar faces frequent natural disasters like floods, which are triggered by climate change. The study also agrees and predicts that more frequent and intense heavy rain makes extreme weather occurrences with increasing time. According to projections, severe rainfall events would increase in frequency and intensity in northern Myanmar. This can have significant impacts on water resources, agriculture, and infrastructure of the study area. Moreover, Myanmar needs to continue studying and monitoring rainfall patterns, develop effective adaptation strategies, and strengthen disaster preparedness to mitigate the impacts of heavy rainfall and ensure sustainable development in the face of climate change. Further research is still needed to understand these changes and their potential impacts on the region's natural disasters.

Data Availability

Reanalysis rainfall and model running data for this study were downloaded from the ECMWF data portal. And this is a fifth-generation ECMWF reanalysis dataset with a geographical resolution of $0.25^{\circ} \times 0.25^{\circ}$ for global climate parameters over the previous decades that are used to support the findings of this study and are included within the article. Data is now freely available from 1950 to the present by registration at ECMWF (https://cds.climate.copernicus.eu/cdsapp#!/dataset/reanalysis-era5-single-levels-monthly-means?tab=form). The actual monthly rainfall observation data from 79 observation stations used to support the findings of this study was provided under permission by Myanmar's Department of Meteorology and Hydrology (DMH) and hence cannot be freely distributed. Requests for access to these data should be made to the Director-General of DMH, Myanmar. Software (https://www.moezala.gov.mm/) and code availability (Open Grads (OpenGrADS - Home)), climate data operator (https://code.mpimet.mpg.de/), python, and IBM SPSS are mainly used for this study. Among these first two are open-source applications for everyone. Codes are available upon reasonable request.

Disclosure

The manuscript was published at preprint server for open access [70].

Conflicts of Interest

I declared that there is no potential conflict of interest with any of the following statements. (1) For any component of the submitted work, the author received no cash or services from a third party (government, commercial, private foundation, etc.) (including but not limited to grants, data monitoring board, study design, manuscript preparation, statistical analysis, etc.). (2) The author is not affiliated with any entity that has a direct or indirect financial interest in the manuscript's subject matter. (3) The author was involved in the following aspects of the project: (a) idea and design, or data analysis and interpretation; (b) authoring the article or critically reviewing it for essential intellectual content; and (c) approval of the final version. (4) This work has not been submitted to and is not currently being reviewed by any other journal or publishing venue. (5) The author has no patents that are broadly relevant to the work, whether proposed, pending, or issued. (6) The author received no payment or services from a third party for any aspect of the submitted work (government, commercial, private foundation, etc.) (including but not limited to grants, data monitoring board, study design, manuscript preparation, statistical analysis, etc.).

Authors' Contributions

Kazora Jonah contributed to the conception and Kyaw Than Oo contributed to the acquisition of data, analysis, and interpretation of data and results; the writing of the manuscript; and the drafting of the article. Chen Haishan supervised and reviewed the manuscript.

Acknowledgments

The author acknowledges the scientists of the ECMFW for supporting ERA5 datasets. The Department of Meteorology and Hydrology (DMH), Myanmar, is also acknowledged for providing the observed rainfall datasets. Also, thanks are due to the Nanjing University of Information Science and Technology (NUIST) for supporting my skills and techniques. I show deep gratitude to Professor Haishan Chen from NUIST, who supervises my PhD study, and Professor Juan Li from NUIST, who supported the basic methods and concepts for this study. Publishing is being carried out using self-funding.

References

[1] Z. M. M. Sein, X. Zhi, I. Ullah et al., "Recent variability of sub-seasonal monsoon precipitation and its potential drivers in Myanmar using in-situ observation during 1981–2020," *International Journal of Climatology*, vol. 42, no. 6, pp. 3341–3359, 2022.

[2] K. T. Oo, "Interannual variability of winter rainfall in upper Myanmar," *Journal of Sustainability and Environmental Management*, vol. 1, no. 3, pp. 344–358, 2022.

[3] K. T. Oo, "Climatology definition of the Myanmar southwest monsoon (MSwM): change point index (CPI)," *Advances in Meteorology*, vol. 2023, Article ID 2346975, 18 pages, 2023.

[4] S. Asia, *Risk Profile Myanmar*, European Commission, 2017.

[5] Z. M. M. Sein, I. Ullah, F. Saleem, X. Zhi, S. Syed, and K. Azam, "Interdecadal variability in Myanmar rainfall in the monsoon season (May–October) using Eigen methods," *Water*, vol. 13, no. 5, 2021.

[6] O. Htway and J. Matsumoto, "Climatological onset dates of summer monsoon over Myanmar," *International Journal of Climatology*, vol. 31, no. 3, pp. 382–393, 2011.

[7] H. M. Thwe, P. Kristiansen, and D. F. Herridge, "Benchmarks for improved productivity and profitability of monsoon rice in lower Myanmar," *Field Crops Research*, vol. 233, pp. 59–69, 2019.

[8] H. M. Fritz, C. Blount, S. Thwin, M. K. Thu, and N. Chan, "Observations and modeling of cyclone Nargis storm surge in Myanmar," in *Solutions to Coastal Disasters 2011*, Anchorage, Alaska, United States, 2011.

[9] E. M. Latrubesse, E. Park, and K. Kastner, "The Ayeyarwady River (Myanmar): washload transport and its global role among rivers in the Anthropocene," *PLoS One*, vol. 16, no. 5, 2021.

[10] E. J. Anthony, M. Besset, P. Dussouillez, M. Goichot, and H. Loisel, "Overview of the monsoon-influenced Ayeyarwady River delta, and delta shoreline mobility in response to changing fluvial sediment supply," *Marine Geology*, vol. 417, 2019.

[11] L. Taft and M. Evers, "A review of current and possible future human-water interactions in Myanmar's river basins," *Hydrology and Earth System Sciences Discussions*, vol. 20, no. 12, 2016.

[12] C. Lesk, P. Rowhani, and N. Ramankutty, "Influence of extreme weather disasters on global crop production," *Nature*, vol. 529, no. 7584, pp. 84–87, 2016.

[13] J. Zhang, C. J. van Westen, H. Tanyas et al., "How size and trigger matter: analyzing rainfall- and earthquake-triggered landslide inventories and their causal relation in the Koshi River basin, central Himalaya," *Natural Hazards and Earth System Sciences*, vol. 19, no. 8, pp. 1789–1805, 2019.

[14] J. B. H. Shyu, C. C. Wang, Y. Wang et al., "Upper-plate splay fault earthquakes along the Arakan subduction belt recorded by uplifted coral microatolls on northern Ramree Island, western Myanmar (Burma)," *Earth and Planetary Science Letters*, vol. 484, pp. 241–252, 2018.

[15] X. Wang, S. Wei, Y. Wang et al., "A 3-D shear wave velocity model for Myanmar region," *Journal of Geophysical Research: Solid Earth*, vol. 124, no. 1, pp. 504–526, 2019.

[16] Department of Meteorology and Hydrology, *Hazard profile of Myanmar*, p. 97, 2009.

[17] C. B. Field, *Managing the Risks of Extreme Events and Disasters to Advance Climate Change Adaptation: Special Report of the Intergovernmental Panel on Climate Change*, Cambridge University Press, 2012.

[18] D. Brill, K. Seeger, A. Pint et al., "Modern and historical tropical cyclone and tsunami deposits at the coast of Myanmar: implications for their identification and preservation in the geological record," *Sedimentology*, vol. 67, no. 3, pp. 1431–1459, 2020.

[19] R. P. Allan and B. J. Soden, "Atmospheric warming and the amplification of precipitation extremes," *Science*, vol. 321, no. 5895, pp. 1481–1484, 2008.

[20] D. S. Arndt, M. O. Baringer, and M. R. Johnson, "State of the climate in 2009," *Bulletin of the American Meteorological Society*, vol. 91, no. 7, pp. s1–s222, 2010.

[21] N. Endo, J. Matsumoto, and T. Lwin, "Trends in precipitation extremes over Southeast Asia," *Scientific Online Letters on the Atmosphere*, vol. 5, no. 1, pp. 168–171, 2009.

[22] P. Bak and C. Tang, "Earthquakes as a self-organized critical phenomenon," *Journal of Geophysical Research: Solid Earth*, vol. 94, no. B11, pp. 15635–15637, 1989.

[23] A. Bhardwaj, S. Singh, L. Sam et al., "A review on remotely sensed land surface temperature anomaly as an earthquake precursor," *International Journal of Applied Earth Observation and Geoinformation*, vol. 63, pp. 158–166, 2017.

[24] M. Wang, Q. Wang, Y. Cai, C. Xu, Z. Zhang, and J. Meng, "Analysis of microseisms caused by storm and typhoon," *Acta Seismologica Sinica*, vol. 40, no. 1, pp. 89–97, 2018.

[25] S. Hainzl, T. Kraft, J. Wassermann, H. Igel, and E. Schmedes, "Evidence for rainfall-triggered earthquake activity," *Geophysical Research Letters*, vol. 33, no. 19, 2006.

[26] P. Steer, L. Jeandet-Ribes, R. Cattin et al., *Towards a better understanding of the impact of erosion on fault slip and seismicity*, EGU General Assembly Conference Abstracts, 2021.

[27] D. R. Caldwell and W. P. Elliott, "Surface stresses produced by rainfall," *Journal of Physical Oceanography*, vol. 1, no. 2, pp. 145–148, 1971.

[28] K. Evans and F. Wyatt, "Water table effects on the measurement of earth strain," *Tectonophysics*, vol. 108, no. 3–4, pp. 323–337, 1984.

[29] R. Hlaing, E. Gunawan, S. Widiyantoro, I. Meilano, and A. Saepuloh, "Assessment of the maximum magnitude of strike-slip faults in Myanmar," *Geotechnical and Geological Engineering*, vol. 37, no. 6, pp. 5113–5122, 2019.

[30] L. S. Huang, J. McRaney, T. L. Teng, and M. Prebish, "A preliminary study on the relationship between precipitation and large earthquakes in Southern California," *Pure and Applied Geophysics PAGEOPH*, vol. 117, no. 6, pp. 1286–1300, 1979.

[31] T. Kraft, J. Wassermann, E. Schmedes, and H. Igel, "Meteorological triggering of earthquake swarms at Mt. Hochstaufen, SE-Germany," *Tectonophysics*, vol. 424, no. 3–4, pp. 245–258, 2006.

[32] H. Goswami, M. Devi, S. Rambabu, A. Barbara, and K. Prakash, *An Analysis of the Relation between Precipitation and Earthquake in the Indian Region*, NISCAIR-CSIR, India, 2014.

[33] D. Zhao, L. Chen, and Y. Yu, "Associations between strong earthquakes and local rainfall in China," *Frontiers in Earth Science*, vol. 9, pp. 1–13, 2021.

[34] G. A. MacRae, U. T. Myint, and S. K. Jain, “Steps in earthquake proofing a country: a case study of Myanmar,” *Bulletin of the New Zealand Society for Earthquake Engineering*, vol. 44, no. 2, pp. 87–98, 2011.

[35] M. Thein, T. Myint, S. T. Tun, and T. L. Swe, “Earthquake and tsunami hazard in Myanmar,” *Journal of Earthquake and Tsunami*, vol. 3, no. 2, pp. 43–57, 2009.

[36] X. Xiong, B. Shan, Y. M. Zhou et al., “Coulomb stress transfer and accumulation on the Sagaing fault, Myanmar, over the past 110 years and its implications for seismic hazard,” *Geophysical Research Letters*, vol. 44, no. 10, pp. 4781–4789, 2017.

[37] Y. Wang, *Earthquake geology of Myanmar*, Diss. California Institute of Technology, 2013, http://resolver.caltech.edu/CaltechTHESIS:06062013-135816595.

[38] M. Nied, T. Pardowitz, K. Nissen, U. Ulbrich, Y. Hundecha, and B. Merz, “On the relationship between hydro-meteorological patterns and flood types,” *Journal of Hydrology*, vol. 519, pp. 3249–3262, 2014.

[39] B. C. Yen, “Urban flood hazard and its mitigation,” in *Urban Disaster Mitigation: The Role of Engineering and Technology*, pp. 245–260, Pergamon, 1995.

[40] Z. M. Khaing, K. Zhang, H. Sawano, B. B. Shrestha, T. Sayama, and K. Nakamura, “Flood hazard mapping and assessment in data-scarce Nyaungdon area, Myanmar,” *PLoS ONE*, vol. 14, no. 11, 2019.

[41] R. Chhin, M. M. Shwe, and S. Yoden, “Time-lagged correlations associated with interannual variations of pre-monsoon and post-monsoon precipitation in Myanmar and the Indochina Peninsula,” *International Journal of Climatology*, vol. 40, no. 8, pp. 3792–3812, 2020.

[42] S. S. Myint and A. A. Thant, “Analysis of rainfall data for selected areas in Myanmar,” *International Journal of Latest Technology in Engineering, Management & Applied Science (IJLTEMAS)*, vol. VIII, no. VIII, pp. 26–32, 2019.

[43] Y. Y. Win, C. Linburt, and Y. Y. May, “Characteristic flora and fauna of the Kachin State, Northern Myanmar,” *Journal of the Myanmar Academy of Arts and Science*, vol. III, no. 4, p. 10, 2005, http://inis.iaea.org/search/search.aspx?orig_q=RN:41086858.

[44] Z. Z. Latt and H. Wittenberg, “Hydrology and flood probability of the monsoon-dominated chindwin river in northern Myanmar,” *Journal of Water and Climate Change*, vol. 6, no. 1, pp. 144–160, 2015.

[45] CFE-DMHA, “Myanmar Disaster Management Reference Handbook,” *Center for Excellence in Disaster Management and Humanitarian Assistance (CFE-DM), Department of Defense*, 2020.

[46] E. Aguilar, T. C. Peterson, P. R. Obando et al., “Changes in precipitation and temperature extremes in Central America and northern South America, 1961-2003,” *Journal of Geophysical Research Atmospheres*, vol. 110, no. D23, pp. 1–15, 2005.

[47] L. L. Aung, *Myanmar climate report*, Norwgian Meterological Institute, 2017.

[48] K. Dang, D. H. Loi, K. Sassa, D. M. Duc, and N. D. Ha, “Hazard Assessment of a Rainfall-Induced Deep-Seated Landslide in Hakha City, Myanmar,” in *Understanding and Reducing Landslide Disaster Risk. WLF 2020. ICL Contribution to Landslide Disaster Risk Reduction*, B. Tiwari, K. Sassa, P. T. Bobrowsky, and K. Takara, Eds., Springer, Cham, 2021.

[49] D. A. Lavers, A. Simmons, F. Vamborg, and M. J. Rodwell, “An evaluation of ERA5 precipitation for climate monitoring,” *Quarterly Journal of the Royal Meteorological Society*, vol. 148, no. 748, pp. 3152–3165, 2022.

[50] A. K. Kyaw, S. Shahid, and X. Wang, “Remote sensing for development of rainfall intensity–duration–frequency curves at ungauged locations of Yangon, Myanmar,” *Water*, vol. 14, no. 11, 2022.

[51] N. L. Win and K. M. Win, “Comparative study of flood frequency analysis on selected rivers in Myanmar,” in *CIEC 2013*, pp. 287–299, Springer, Singapore, 2014.

[52] A. Al, M. Noor, and H. Mohamad, “Estimation of short-duration rainfall intensity from daily rainfall values in Klang Valley, Malaysia,” *Applied Water Science*, vol. 8, no. 7, pp. 1–10, 2018.

[53] M. S. Shamkhi, M. K. Azeez, and Z. H. Obeid, “Deriving rainfall intensity-duration-frequency (IDF) curves and testing the best distribution using EasyFit software 5.5 for Kut city, Iraq,” *Open Engineering*, vol. 12, no. 1, pp. 834–843, 2022.

[54] E. S. Mahdi and M. Z. Mohamedmeki, “Analysis of rainfall intensity-duration-frequency (IDF) curves of Baghdad city,” *IOP Conference Series: Materials Science and Engineering*, vol. 888, no. 1, 2020.

[55] Y. Sun, D. Wendi, D. E. Kim, and S. Y. Liong, “Deriving intensity–duration–frequency (IDF) curves using downscaled in situ rainfall assimilated with remote sensing data,” *Geoscience Letters*, vol. 6, no. 1, 2019.

[56] E. J. Gumbel, *Statistics of Extremes*, Columbia University Press, New York Chichester, West Sussex, 1958.

[57] V. Te Chow, D. R. Maidment, and L. W. Mays, *Chow's Handbook of Applied Hydrology*, McGraw-Hill Education, U.S, 1988.

[58] V. P. Singh, “Log-Pearson type III distribution,” *Entropy-Based Parameter Estimation in Hydrology*, vol. 3, no. 1967, pp. 252–274, 1998.

[59] I. H. Elsebaie, “Developing rainfall intensity-duration-frequency relationship for two regions in Saudi Arabia,” *Journal of King Saud University: Engineering Sciences*, vol. 24, no. 2, pp. 131–140, 2012.

[60] S. L. Sørland, R. Brogli, P. K. Pothapakula et al., “COSMO-CLM regional climate simulations in the coordinated regional climate downscaling experiment (CORDEX) framework: a review,” *Geoscientific Model Development*, vol. 14, no. 8, pp. 5125–5154, 2021.

[61] K. Riahi, D. P. van Vuuren, E. Kriegler et al., “The shared socioeconomic pathways and their energy, land use, and greenhouse gas emissions implications: an overview,” *Global Environmental Change*, vol. 42, pp. 153–168, 2017.

[62] P. Mote, L. Brekke, P. B. Duffy, and E. Maurer, “Guidelines for constructing climate scenarios,” *Eos*, vol. 92, no. 31, pp. 257-258, 2011.

[63] T. Karl, N. Nicholls, and A. Ghazi, *Weather and climate extremes: changes, variations, and a perspective from the insurance industry*, Springer Science & Business Media, 1999.

[64] X. Zhang, G. Hegerl, F. W. Zwiers, and J. Kenyon, “Avoiding inhomogeneity in percentile-based indices of temperature extremes,” *Journal of Climate*, vol. 18, no. 11, pp. 1641–1651, 2005.

[65] W. Kirch, Ed., “Pearson's correlation coefficient,” in *Encyclopedia of Public Health*, pp. 1090-1091, Springer Netherlands, Dordrecht, 2008.

[66] M. T. Toe, M. Kanzaki, T.-H. Lien, and K.-S. Cheng, “Spatial and temporal rainfall patterns in {central} {dry} {zone},

{Myanmar} - {a} hydrological cross-scale analysis," *Terrestrial, Atmospheric and Oceanic Sciences*, vol. 28, no. 3, pp. 425–436, 2017.

[67] Z. M. M. Sein, X. Zhi, F. K. Ogou, I. K. Nooni, K. T. C. L. K. Sian, and G. T. Gnitou, "Spatio-temporal analysis of drought variability in Myanmar based on the standardized precipitation evapotranspiration index (SPEI) and its impact on crop production," *Agronomy*, vol. 11, no. 9, p. 1691, 2021.

[68] B. C. O'Neill, C. Tebaldi, D. P. Van Vuuren et al., "The scenario model intercomparison project (ScenarioMIP) for CMIP6," *Geoscientific Model Development*, vol. 9, no. 9, pp. 3461–3482, 2016.

[69] Intergovernmental Panel on Climate Change (IPCC), "Climate resilient development pathways," in *Climate Change 2022 – Impacts, Adaptation and Vulnerability*, pp. 2655–2808, IPCC, 2023.

[70] K. J. K. T. Oo, *Climate Change Impact on the Trigger of Natural Disasters over East Southeastern Himalayas Foothill Region of Myanmar: Extreme Rainfall Analysis*, Research Square, 2023.